Axle charge effects on photoinduced electron transfer processes in rotaxanes containing porphyrin and [60]fullerene†

Hisahiro Sasabe,[ab] Atula S. D. Sandanayaka,[cd] Nobuhiro Kihara,[be] Yoshio Furusho,[bf] Toshikazu Takata,*[bg] Yasuyuki Araki[d] and Osamu Ito*[d]

Received 13th July 2009, Accepted 9th September 2009
First published as an Advance Article on the web 5th October 2009
DOI: 10.1039/b913966d

Two rotaxanes containing zinc porphyrin (ZnP) with crown ether and [60]fullerene (C_{60}) with cationic and neutral axles are synthesized. Optimized structures calculated by molecular orbital methods indicate that the rotaxane with an ammonium cation in the center of the axle has a shorter distance between the C_{60} and ZnP moieties than that of the rotaxane with a neutral axle because of acylation of the ammonium cation, which draws away the C_{60} and ZnP moieties by releasing the interaction with the crown ether. The charge-transfer interaction is revealed by absorption spectra for the rotaxane with a short distance, but not for the rotaxane with a long distance, which strongly affects the rates and efficiencies of photoinduced electron-transfer and energy-transfer processes *via* the excited singlet states of the ZnP and C_{60} moieties and their triplet states, as revealed by the time-resolved fluorescence and absorption measurements. The rate of the charge recombination of the radical ion pair of the rotaxane with a neutral axle is slower than that of the rotaxane with a cationic axle, due to the loose structure of the former rotaxane, which results from the long distance between the C_{60} anion radical and the ZnP cation radical.

Introduction

Donor–acceptor rotaxane molecules have emerged as novel supramolecules in artificial photosynthetic devices and nanoscale devices.[1,2] Synthesized rotaxane molecules containing various donors and acceptors undergo photoinduced electron transfer (PET) to produce high charge-separated states with high quantum yields.[3] These properties depend on the length of the spatial distance between the donor and acceptor in the rotaxane. Information acquired from the investigations of such rotaxane molecules is of interest not only in realizing photosynthesis models, but also in designing optoelectronic systems.[4]

Among such rotaxanes, [60]fullerenes have been widely employed as electron acceptors.[5–8] In our previous reports,[9] it has been revealed that the length of the axle tethered through the ring appending fullerene is important to control the spatially positioned donors with respect to the fullerenes. When ferrocene (Fc) was used as electron-donor in these fullerene rotaxanes, the relative spatial position is controlled with the axle charge;[10] however, the interaction between the C_{60} and Fc moieties is not strong enough to show charge-transfer (CT) interaction in the ground state.

In the present study, we design two rotaxanes using zinc porphyrin (ZnP) as an electron donor with respect to the C_{60} moiety; the relative position between them is controlled by the chemical reaction on the axle as shown in Scheme 1, expecting that the strength of the CT interaction simultaneously changes with the distance between the ZnP and C_{60} moieties.

The synthesized two rotaxanes have the ZnP moiety with crown ether, through which the axle with the C_{60} moiety reeves. In Scheme 1, the method to convert a rotaxane with an ammonium cation in the center of the axle ($\mathbf{((C_{60}(N^+);ZnP)_{Rot}}$) to another rotaxane with a neutral axle ($\mathbf{((C_{60}(N);ZnP)_{Rot}}$) is shown. In the case of $\mathbf{(C_{60}(N^+);ZnP)_{Rot}}$, the positive charge of the N atom in the middle of the axle fixes in the center of crown ether so as to place the ZnP plane in a limited spatial arrangement with respect to the C_{60} sphere, appropriate for strong CT interaction between them. For newly synthesized $\mathbf{(C_{60}(N);ZnP)_{Rot}}$ in the present study, the relatively longer distance between the ZnP moiety and the C_{60} moiety would be expected by the introduction of the benzoyl group on the N atom along with withdrawal of the center of the axle to the crown ether, which draws away the C_{60} moiety from the ZnP moiety, removing the CT interaction.

[a] *Department of Organic Device Engineering, Yamagata University, 4-3-16 Jonan, Yonezawa, Yamagata, 992-8510, Japan E-mail: h-sasabe@yz.yamagata-u.ac.jp*
[b] *Department of Applied Chemistry, Osaka Prefecture University, Sakai, 599-8531, Japan*
[c] *Japan Advanced Institute of Science and Technology, Asahidai, Nomi, 923-1292, Japan. E-mail: sandanay@jaist.ac.jp*
[d] *IMRAM, Tohoku University, Katahira 2-1-1, Aoba-ku, Sendai, 980-8577 Japan. E-mail: ito@tagen.tohoku.ac.jp*
[e] *Department of Chemistry, Kanagawa University, Tsuchiya, Hiratsuka 259-1293, Japan. E-mail: kihara@kanagawa-u.ac.jp*
[f] *Department of Molecular Design and Engineering, Nagoya University, Japan. E-mail: furusho@apchem.nagoya-u.ac.jp*
[g] *Department of Organic and Polymeric Materials, Tokyo Institute of Technology, Ookayama, Meguro-ku, 152-8552, Tokyo, Japan. E-mail: ttakata@polymer.titech.ac.jp*

† Electronic supplementary information (ESI) available: Molecular structures; free energy data; cyclic voltammograms; fluorescence spectra; transient absorption spectra. See DOI: 10.1039/b913966d

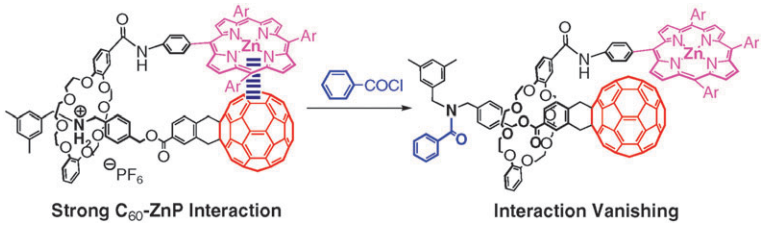

Scheme 1 Molecular structures of the rotaxane with a cationic axle (abbreviated as $(C_{60}(N^+);ZnP)_{Rot}$ and the rotaxane with a neutral axle $(C_{60}(N);ZnP)_{Rot}$, and their conversion reaction with benzoyl chloride.

For these two synthesized rotaxanes, we investigate differences of the PET processes using the time-resolved transient absorption and fluorescence measurements with changing solvent polarity. Furthermore, it would be important to compare the PET processes of the covalently connected C_{60}-donor systems[11] and other supramolecular systems[12] with the newly synthesized rotaxanes, in which the through-space ET would be expected to predominate.[9]

Results and discussion

Synthesis of rotaxanes

$(C_{60}(N);ZnP)_{Rot}$ was synthesized with acylation of $(C_{60}(N^+);ZnP)_{Rot}$[13] using benzoyl chloride (Scheme 1). The structures of these rotaxanes were fully characterized by the MALDI-TOF-MS, NMR, IR and UV-vis spectra along with elemental analysis as described in the Experimental section.

Optimized structures and molecular orbitals

Optimized structures of both rotaxanes were evaluated by the molecular orbital calculations with the *Gaussian ab initio* B3LYP/3-21G(*)s dynamic method.[14] Since many structures with minimal energies were given due to the fluctuation of each rotaxane molecule,[15] a typical structure with minimal energy is shown in Fig. 1 as an example of optimized structures. The HOMO and LUMO calculated with *ab initio* B3LYP/3-21G(*)[14] are superposed on these optimized structures.

In the case of $(C_{60}(N^+);ZnP)_{Rot}$, the distance between the C_{60} sphere and the ZnP plane is quite short, showing an approach as if the ZnP plane accommodates the C_{60} ball, suggesting a considerable interaction between the ZnP and C_{60} moieties. On the other hand, in the case of $(C_{60}(N);ZnP)_{Rot}$, the distance becomes long and the ZnP plane positions perpendicularly with respect to the C_{60} sphere.

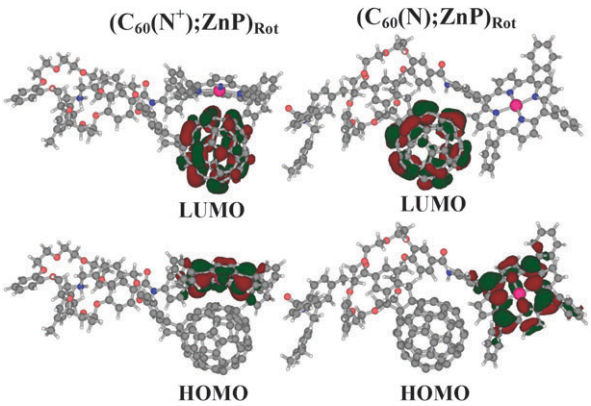

Fig. 1 Optimized structure, HOMO and LUMO of $(C_{60}(N^+);ZnP)_{Rot}$ and $(C_{60}(N);ZnP)_{Rot}$ calculated with *ab initio* B3LYP/3-21G(*).

In both rotaxanes, the electron densities of the HOMO are localized predominantly on the ZnP entity, whereas those of the LUMO are localized on the C_{60} sphere, suggesting the most stable radical ion pair structure, such as $(C_{60}^{\bullet-}(N);ZnP^{\bullet+})_{Rot}$ or $(C_{60}^{\bullet-}(N^+);ZnP^{\bullet+})_{Rot}$.

Although a spread of a small amount of electron density of the HOMO and LUMO over both C_{60} and ZnP moieties in $(C_{60}(N^+);ZnP)_{Rot}$ is observed, as would be expected due to the CT interaction, appreciable delocalization was not seen in Fig. 1. This is interpreted by the delocalization of the transferred small amount of charge all over the large ZnP plane and C_{60} sphere, which dilutes the electron densities of these frontier MOs in Fig. 1.

The average center-to-center distances (R_{CC}^{Av}) between the C_{60} and ZnP moieties for $(C_{60}(N);ZnP)_{Rot}$ and $(C_{60}(N^+);ZnP)_{Rot}$ were evaluated to be 11.0 and 6.7 Å, respectively. This suggests that a close contact between the ZnP plane and the C_{60} sphere in $(C_{60}(N^+);ZnP)_{Rot}$ allows the CT interaction. In the excited states, such difference in the R_{CC}^{Av} values between $(C_{60}(N);ZnP)_{Rot}$ and $(C_{60}(N^+);ZnP)_{Rot}$ would strongly affect the PET process.

Steady-state absorption spectra

The absorption spectra of $(C_{60}(N);ZnP)_{Rot}$ in toluene are shown in Fig. 2a with reference compounds (see the ESI, Scheme S1†). The Soret-band and Q-bands of the ZnP moiety in this rotaxane appear at 427 and 552–592 nm, respectively. The absorption bands of the C_{60} moiety appeared at 705 nm and in the shorter wavelength than 350 nm. The absorption spectrum of the rotaxane is almost a superimposition of those of references.

Interestingly, for $(C_{60}(N^+);ZnP)_{Rot}$ (Fig. 2b), a new weak broad band in the 750–850 nm region was observed, indicating CT interaction in the ground state, which supports experimentally the optimized structures obtained with the MO calculations. In addition, red shifts of the Soret and Q bands of the ZnP moiety by about 6 nm were observed, supporting the CT interaction.

Electrochemical studies

The free energies of the CS-processes for the generations of $(C_{60}^{\bullet-}(N);ZnP^{\bullet+})_{Rot}$, and $(C_{60}^{\bullet-}(N^+);ZnP^{\bullet+})_{Rot}$ were estimated using the data obtained from electrochemical measurements. Thus, the cyclic voltammograms were measured in PhCN solution containing n-$(C_4H_9)_4NPF_6$ as a supporting electrolyte (ESI; Fig. S1†). The first oxidation

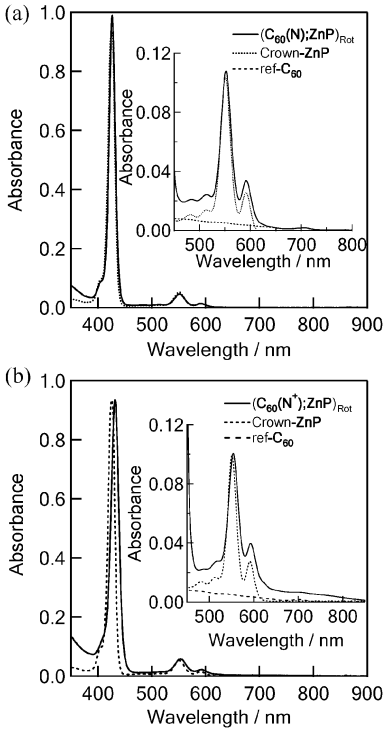

Fig. 2 Steady-state absorption spectra of (upper panel) **$(C_{60}(N);ZnP)_{Rot}$** and (lower panel) **$(C_{60}(N^+);ZnP)_{Rot}$** in toluene (concentration = 0.005 mM). Inset: the vertical axis is magnified by 10 times. Structure of Crown-**ZnP** and ref-C_{60}; see ESI.†

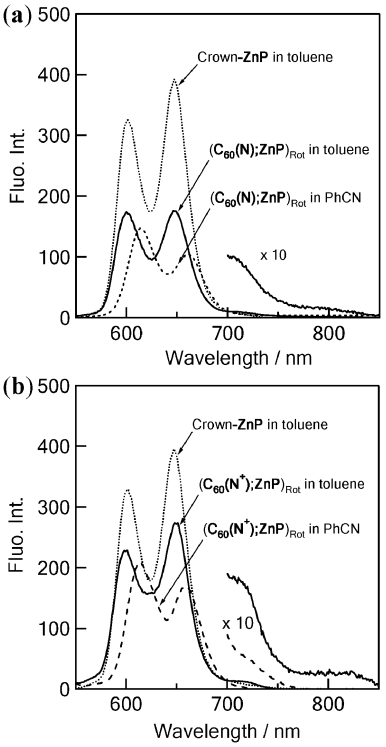

Fig. 3 Steady-state fluorescence spectra of (a) **$(C_{60}(N);ZnP)_{Rot}$**, (b) **$(C_{60}(N^+);ZnP)_{Rot}$** in toluene (—) and PhCN (---); concentrations are all 0.1 mM, which normalizes the absorbance at λ_{ex} = 550 nm.

potentials (E_{Ox}) and first reduction (E_{Red}) are attributed to those of the C_{60} and ZnP moieties, respectively; E_{Ox} = 0.29 V and E_{Red} = −1.00 V *vs* Fc/Fc^+ in Ar-saturated PhCN, giving the electrochemical HOMO–LUMO gap = 1.29 eV for **$(C_{60}(N);ZnP)_{Rot}$**; similarly, for **$(C_{60}(N^+);ZnP)_{Rot}$**, E_{Ox} = 0.22 V, E_{Red} = −1.06 V and the HOMO–LUMO gap = 1.28 eV. Both rotaxanes have similar electrochemical data within 0.07 V.

The free-energy changes of the CS process (ΔG_{CS}) were calculated using these data by the Rehm–Weller equation.[16] The ΔG_{CS} values *via* ^{1}ZnP* ($\Delta G_{CS}^{S\,I}$) and ^{3}ZnP* ($\Delta G_{CS}^{T\,I}$) *vs* C_{60} are all negative in polar solvents as listed in Table 1, predicting that both CS processes are possible for both rotaxanes. Even in nonpolar toluene, the CS process from ^{3}ZnP* is also possible for **$(C_{60}(N^+);ZnP)_{Rot}$**. The ΔG_{CS} values *via* $^1C_{60}$* ($\Delta G_{CS}^{S\,II}$) and $^3C_{60}$*, ($\Delta G_{CS}^{T\,II}$) are negative only in polar solvents, suggesting that both CS processes are also possible processes for both rotaxanes. In nonpolar solvent, the $\Delta G_{CS}^{T\,II}$ values for both rotaxanes are slightly positive, predicting the difficulty of the CS process in nonpolar solvents. The free-energy changes of the charge recombination process (ΔG_{CR}) are equal to those of the radical ion-pairs (ΔG_{RIP}); they decrease with solvent polarity from 1.7 eV (toluene) to 1.2 eV (DMF) for both rotaxanes (these values are listed in the ESI; Table S1†).

Steady-state fluorescence studies

In order to reveal the photoexcited properties, the steady-state fluorescence spectra of both rotaxanes were measured with using 550-nm light, which selectively excites the ZnP moiety (Fig. 3). The fluorescence peaks at 600 and 650 nm are attributed to that of the ZnP moiety in the rotaxanes, judging from the fluorescence peak of Crown-**ZnP**. The ZnP-fluorescence intensities of these rotaxanes are weaker than that of Crown-**ZnP**, indicating the quenching of the ^{1}ZnP* moiety by the C_{60} moiety; *ca.* 50% quenching for **$(C_{60}(N);ZnP)_{Rot}$** and *ca.* 30% quenching for **$(C_{60}(N^+);ZnP)_{Rot}$**. In toluene, the C_{60}-fluorescence peak clearly appears at 715 nm, suggesting energy transfer (EnT) from the ^{1}ZnP* moiety to the C_{60} moiety. On the other hand, in polar solvents such as PhCN, the fluorescence peak of the $^1C_{60}$* moiety was not appreciably observed as shown in Fig. 3b, suggesting that the CS process takes place *via* the ^{1}ZnP* moiety and successively *via* the $^1C_{60}$* moiety.

In the case of **$(C_{60}(N^+);ZnP)_{Rot}$**, in addition to the C_{60}-fluorescence at 715 nm, weak fluorescence appears in the 750–850 nm region (Fig. 3b), which can be attributed to the CT-fluorescence of the excited complex between the ZnP with C_{60} moieties.[17]

These observations indicate that the fractions of the EnT and CS processes *via* the ^{1}ZnP* moiety depend on the solvent polarity. In addition, the CS process *via* the $^1C_{60}$* moiety is also possible in polar solvents. Furthermore, the CT interaction also contributes to the excited state of **$(C_{60}(N^+);ZnP)_{Rot}$**.

Time-resolved fluorescence studies

The fluorescence time profiles of the ZnP-fluorescence in both rotaxanes were measured using time-correlated single-photon-counting apparatus with excitation at 410 nm (Fig. 4), which

Table 1 Free–energy changes of charge-separation (ΔG^{S}_{CS}) for **(C$_{60}$(N$^+$);ZnP)$_{Rot}$** and **(C$_{60}$(N);ZnP)$_{Rot}$**

Rotaxanes	Solvent	$\Delta G^{S}_{CS}{}^{I}$/eV (*via* ^{1}ZnP* *vs* C$_{60}$)	$\Delta G^{S}_{CS}{}^{II}$/eV (*via* ^{1}C$_{60}$* *vs* ZnP)	$\Delta G^{T}_{CS}{}^{II}$/eV (*via* ^{3}C$_{60}$* *vs* ZnP)
(C$_{60}$(N);ZnP)$_{Rot}$	DMF	−0.78	−0.53	−0.31
	PhCN	−0.76	−0.51	−0.29
	THF	−0.63	−0.38	−0.16
	TN	−0.21	0.04	0.26
(C$_{60}$(N$^+$);ZnP)$_{Rot}$	DMF	−0.93	−0.58	−0.36
	PhCN	−0.91	−0.56	−0.34
	THF	−0.85	−0.50	−0.28
	TN	−0.55	−0.20	0.02

[a] $-\Delta G_{CR} = -E_{Ox} + E_{Red} - \Delta G_S$; and $\Delta G^{S,T}_{CS} = E_{o,o} - \Delta G_{CR}$; $\Delta G^{S}_{CS}{}^{I}$, and $\Delta G^{S}_{CS}{}^{II}$ are CS *via* ^{1}ZnP* and ^{1}C$_{60}$*, respectively; $E_{o,o}$ (^{1}ZnP* = 2.1 eV, ^{3}ZnP* = 1.5 eV; ^{1}C$_{60}$* = 1.75 eV, ^{3}C$_{60}$* = 1.5 eV); $\Delta G_S = e^2/(4\pi\varepsilon_0))[(1/(2R_+) + 1/(2R_-) - 1/R_{CC})/\varepsilon_S - (1/(2R_+) + 1/(2R_-))/\varepsilon_R]$, where R_+ and R_- and R^{Av}_{CC} are radii of radical cation (5 Å) and radical anion (4 Å), and R^{Av}_{CC} = 11.0 Å for **(C$_{60}$(N);ZnP)$_{Rot}$** and R^{Av}_{CC} = 6.7 Å for **(C$_{60}$(N$^+$);ZnP)$_{Rot}$**. The ε_S and ε_R are dielectric constants of solvents used for photophysical studies and for measuring the redox potentials, respectively.[16]

show shortening of the ZnP-fluorescence lifetimes (τ_f). The values of τ_f were evaluated by curve-fitting with single exponential as summarized in Table 2. The τ_f values of both rotaxanes are shorter than that of Crown-**ZnP** (τ_{f0} = 2000 ps), suggesting that dynamic ZnP-fluorescence quenching occurs in all solvents. The τ_f values decrease on going from **(C$_{60}$(N);ZnP)$_{Rot}$** to **(C$_{60}$(N$^+$);ZnP)$_{Rot}$** and increase in the order of DMF > PhCN > THF > toluene in both rotaxanes.

The quenching rates (k_q) and quenching quantum yields (Φ_q) can be evaluated from eqn (1) and (2);[18]

$$k_q = (1/\tau_f) - (1/\tau_{f0}) \quad (1)$$

$$\Phi_q = [(1/\tau_f) - (1/\tau_{f0})]/(1/\tau_f) \quad (2)$$

In toluene, the shorter τ_f values of both rotaxanes (890 and 1440 ps) can be predominantly assigned to the EnT process from the ^{1}ZnP* moiety to the C$_{60}$ moiety; thus, the k_q and Φ_q values can be considered equal to k_{EnT} and Φ_{EnT}, respectively; for **(C$_{60}$(N);ZnP)$_{Rot}$**, k_{EnT} = 6.3 × 10^8 s^{-1} and for **(C$_{60}$(N$^+$);ZnP)$_{Rot}$**, k_{EnT} = 1.9 × 10^8 s^{-1}. The order of k_{EnT} and Φ_{EnT} **(C$_{60}$(N);ZnP)$_{Rot}$** > **(C$_{60}$(N$^+$);ZnP)$_{Rot}$** is opposite to that expected from R^{Av}_{CC}. The small k_{EnT} for **(C$_{60}$(N$^+$);ZnP)$_{Rot}$** suggests that the equilibrium between the **(C$_{60}$(N$^+$);^{1}ZnP*)$_{Rot}$** and the CS state near-by **^{1}C$_{60}$***-state induces slow-down of k_{EnT}.

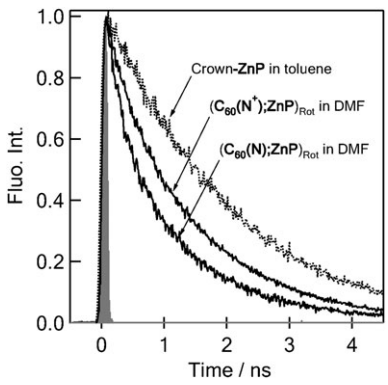

Fig. 4 Time profiles of the ZnP-fluorescence at 625 nm of **(C$_{60}$(N);ZnP)$_{Rot}$**, **(C$_{60}$(N$^+$);ZnP)$_{Rot}$** and Crown-**ZnP** in DMF and toluene; λ_{ex} = 410 nm.

Table 2 Fluorescence lifetimes (τ_f), rate constants (k^S_{CS}, k_{EnT}), and quantum yields (Φ^S_{CS}, Φ_{EN}) for charge separation and energy transfer *via* the ^{1}ZnP* moiety of **(C$_{60}$(N);ZnP)$_{Rot}$** and **(C$_{60}$(N$^+$);ZnP)$_{Rot}$**

Rotaxanes	Solvent	τ_f/ps	k_q/s^{-1}[a]	Φ_q[a]
(C$_{60}$(N);ZnP)$_{Rot}$	DMF	740	8.6 × 10^8	0.63
	PhCN	780	7.9 × 10^8	0.61
	THF	870	9.2 × 10^8	0.57
	TN	890	6.3 × 10^8 (EnT)[b]	0.56 (EnT)[b]
(C$_{60}$(N$^+$);ZnP)$_{Rot}$	DMF	1270	2.8 × 10^8	0.37
	PhCN	1330	2.5 × 10^8	0.34
	THF	1400	2.1 × 10^8	0.30
	TN	1440	1.9 × 10^8 (EnT)[b]	0.27 (EnT)[b]

[a] Lifetime (τ_{f0}) of reference Crown-**ZnP** (τ_{f0} = 2.00 ns in toluene). [b] Predominantly EnT, others include CS and EnT.

To confirm the EnT process, time-resolved emission spectra of **(C$_{60}$(N);ZnP)$_{Rot}$** were observed in toluene; the C$_{60}$-fluorescence appears at 720 nm after the decay of the ZnP-fluorescence around 650 nm, supporting the EnT process *via* the ^{1}ZnP* moiety generates the ^{1}C$_{60}$* moiety. From the rise of the ^{1}C$_{60}$* moiety shown in Fig. 5, the k_{EnT} value was evaluated to be *ca.* 6 × 10^8 s^{-1}, which is in good agreement with that evaluated from the decay of the ^{1}ZnP* moiety, confirming no CS *via* the ^{1}ZnP* moiety in toluene.

In polar solvents, further short τ_f values of the ^{1}ZnP* moiety were evaluated, suggesting that the CS process additionally takes place *via* the ^{1}ZnP* moiety. Therefore, the k_q and Φ_q values may include $k^S{}_{CS}{}^{I}$ and $\Phi^S{}_{CS}{}^{I}$ in addition to k_{EnT} and

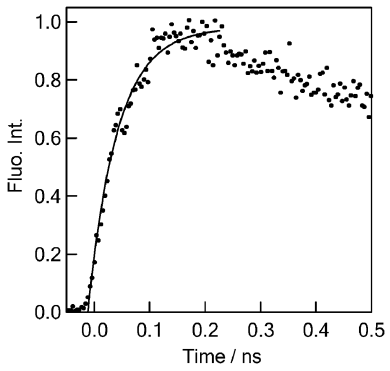

Fig. 5 Time profile of the C$_{60}$-fluorescence at 720 nm for **(C$_{60}$(N);ZnP)$_{Rot}$** in toluene; λ_{ex} = 410 nm.

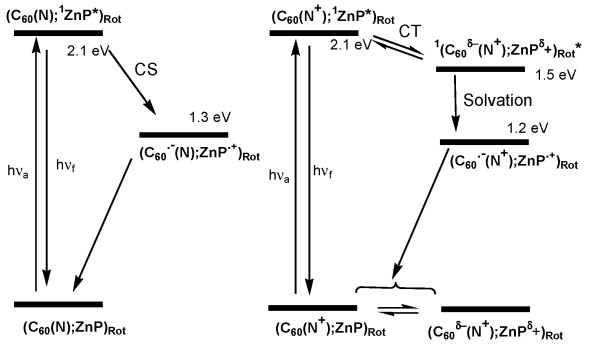

Scheme 2 Decay processes of the ^{1}ZnP* moiety for $\mathbf{(C_{60}(N);ZnP)_{Rot}}$ and $\mathbf{(C_{60}(N^+);ZnP)_{Rot}}$ in polar solvents.

Φ_{EnT} (in these notations, suffix "S" implies "singlet" and "I" implies "*via* ^{1}ZnP*"). The values of ($k^S_{CS}{}^I + k_{EnT}$) are in the range of (8–9) $\times$ 10^8 s^{-1} for $\mathbf{(C_{60}(N);ZnP)_{Rot}}$ and (2–3) $\times$ 10^8 s^{-1} for $\mathbf{(C_{60}(N^+);ZnP)_{Rot}}$; both values are comparable with the intersystem crossing (ISC) to the ^{3}ZnP* moiety. The values of ($\Phi^S_{CS}{}^I + \Phi_{EnT}$) are *ca.* 0.6 and *ca.* 0.3, respectively (Table 2). Remaining quantum yields ($1 - (\Phi^S_{CS}{}^I + \Phi_{EnT})$) may be that of intersystem crossing (Φ_{ISC}) *via* the ^{1}ZnP* moiety. In each rotaxane, these kinetic parameters vary only slightly with solvent polarity. These parameters for $\mathbf{(C_{60}(N);ZnP)_{Rot}}$ are larger than those of $\mathbf{(C_{60}(N^+);ZnP)_{Rot}}$, although the opposite tendency is anticipated from the order of $R^{Av}_{CC}\mathbf{(C_{60};ZnP)_{Rot}} > R^{Av}_{CC}\mathbf{(C_{60}(N^+);ZnP)_{Rot}}$. In the case of $\mathbf{(C_{60}(N^+);ZnP)_{Rot}}$, the CS process may take place *via* the excited CT state, $\mathbf{^1(C_{60}{}^{\delta-}(N^+);ZnP^{\delta+})^*_{Rot}}$, after equilibrium with the excited singlet state $\mathbf{(C_{60}(N^+);{}^1ZnP^*)_{Rot}}$ (Scheme 2). In order to convert the CT state to the CS state $\mathbf{(C_{60}{}^{\bullet-}(N^+);ZnP^{\bullet+})_{Rot}}$, a considerable solvation to stabilize the CS state is necessary, which may slow down the rates of the total CS process *via* ^{1}ZnP*.

The decays of the C_{60}-fluorescence at 720 nm are also accelerated in both rotaxanes (see ESI: Fig. S3†). The C_{60}-fluorescence lifetimes were analyzed by the curve-fitting with a bi-exponential function. The shorter C_{60}-fluorescence lifetimes with the 85–95% fraction are listed in Table 3. For $\mathbf{(C_{60}(N^+);ZnP)_{Rot}}$, shortening of the C_{60}-fluorescence lifetime was observed even in toluene, whereas for $\mathbf{(C_{60}(N);ZnP)_{Rot}}$ the C_{60}-fluorescence lifetime was the same as that of Ref-C_{60} compounds in this nonpolar solvent. Shortening of the C_{60}-fluorescence lifetime indicates that the CS process pre dominantly takes place *via* the $^1C_{60}$* moiety *vs* the ZnP moiety, giving $\mathbf{(C_{60}{}^{\bullet-}(N);ZnP^{\bullet+})_{Rot}}$ and $\mathbf{(C_{60}{}^{\bullet-}(N^+);ZnP^{\bullet+})_{Rot}}$.

Table 3 Fluorescence lifetimes of $^1C_{60}$* (τ_f), rate constant ($k^S_{CS}{}^{II}$) and quantum yield ($\Phi^S_{CS}{}^{II}$) for charge separation *via* $^1C_{60}$* of $\mathbf{(C_{60}(N);ZnP)_{Rot}}$ and $\mathbf{(C_{60}(N^+);ZnP)_{Rot}}$

Rotaxanes	Solvent	τ_f/ps $^1C_{60}$*	$k^S_{CS}{}^{IIa}/s^{-1}$	$\Phi^S_{CS}{}^{IIa}$
$\mathbf{(C_{60}(N);ZnP)_{Rot}}$	DMF	130	7.2×10^9	0.91
	PhCN	180	4.9×10^9	0.87
	THF	260	3.1×10^9	0.81
	TN	1400	—	—
$\mathbf{(C_{60}(N^+);ZnP)_{Rot}}$	DMF	200	4.2×10^9	0.85
	PhCN	230	3.6×10^9	0.83
	THF	490	1.3×10^9	0.63
	TN	500	1.3×10^9	0.63

[a] Lifetime (τ_{f0}) of ref-$\mathbf{C_{60}}$ was 1350 ps in toluene. The $k^S_{CS}{}^{II}$ and $\Phi^S_{CS}{}^{II}$ were calculated from eqn (1) and (2). [b] Longer lifetimes are 800–1400 ps with fraction of 5–15%.

From the τ_f values of the C_{60}-fluorescence, the rate constants ($k^S_{CS}{}^{II}$) and quantum yields ($\Phi^S_{CS}{}^{II}$) of the CS process were evaluated as summarized in Table 3. In each rotaxane, the $k^S_{CS}{}^{II}$ and $\Phi^S_{CS}{}^{II}$ values increase with the solvent polarity. For $\mathbf{(C_{60}(N);ZnP)_{Rot}}$, the $k^S_{CS}{}^{II}$ values are in the range of (3.1–7.2) $\times$ 10^9 s^{-1} and the $\Phi^S_{CS}{}^{II}$ values are in the range of 0.8–0.9 in polar solvents. For $\mathbf{(C_{60}(N^+);ZnP)_{Rot}}$, the $k^S_{CS}{}^{II}$ values are in the range of (1.3–4.2) $\times$ 10^9 s^{-1} and the $\Phi^S_{CS}{}^{II}$ values are in the range of 0.6–0.9, indicating that the $k^S_{CS}{}^{II}$ value for $\mathbf{(C_{60}(N);ZnP)_{Rot}}$ is larger than the corresponding one for $\mathbf{(C_{60}(N^+);ZnP)_{Rot}}$. This tendency is in agreement with that of the $k^S_{CS}{}^I$ values. In toluene, on the other hand, an opposite tendency was found; that is, the CS process *via* the $^1C_{60}$* moiety takes place for $\mathbf{(C_{60}(N^+);ZnP)_{Rot}}$, whereas no CS process for $\mathbf{(C_{60}(N);ZnP)_{Rot}}$. This latter tendency in the $k^S_{CS}{}^{II}$ values is in agreement with the expected one from $R^{Av}_{CC}\mathbf{(C_{60}(N);ZnP)_{Rot}} > R^{Av}_{CC}\mathbf{(C_{60}(N^+);ZnP)_{Rot}}$.

Time-resolved transient absorption studies

Time-resolved transient absorption spectra of both rotaxanes in deaerated PhCN were measured following nanosecond laser excitation (6 ns laser pulse) at 550 nm as shown in Fig. 6. Both rotaxanes show similar features; photo-excitation of the ZnP moiety at 430 nm and of the C_{60} moiety at 532 nm also gave almost the same transient spectra.

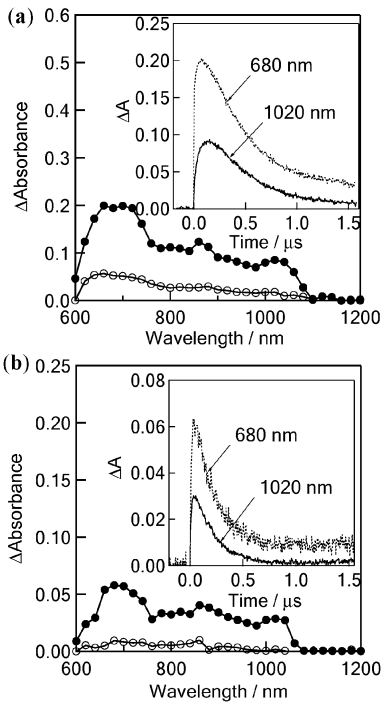

Fig. 6 Nanosecond transient absorption spectra of (a) $\mathbf{(C_{60}(N);ZnP)_{Rot}}$ and (b) $\mathbf{(C_{60}(N^+);ZnP)_{Rot}}$ (0.1 mM) in Ar-saturated PhCN observed by 550 nm laser irradiation in at 0.1 μs (●) and 1.0 μs (○). Inset: Absorption-time profiles at room temperature.

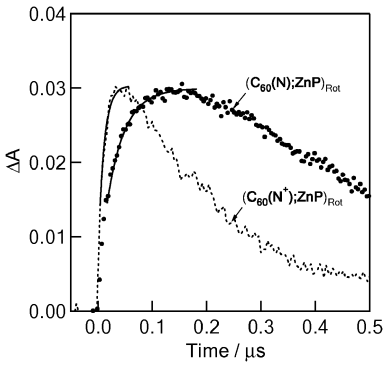

Fig. 7 Absorbance traces of the $C_{60}^{\bullet-}$ moiety at 1020 nm of $\mathbf{(C_{60}(N);ZnP)_{Rot}}$ and $\mathbf{(C_{60}(N^+);ZnP)_{Rot}}$ (0.1 mM) in Ar-saturated PhCN at room temperature (absorbance is normalized as 0.03).

The absorption band at 1020 nm observed immediately after laser pulse was assigned to the $C_{60}^{\bullet-}$ moiety,[9,11] whereas the absorption bands at 700 and 880 nm are assigned to the $^3C_{60}$* and ^{3}ZnP* moiety, respectively. The broad transient absorption in the 640–680 nm region can be attributed to the $ZnP^{\bullet+}$ moiety,[9,11] which may be overlapped with the depression of the ZnP moiety. Similar results were also observed in DMF and THF for both rotaxanes. These results clearly support the generation of the RIPs, $\mathbf{(C_{60}^{\bullet-}(N);ZnP^{\bullet+})_{Rot}}$ and $\mathbf{(C_{60}^{\bullet-}(N^+);ZnP^{\bullet+})_{Rot}}$.

The time profile of the absorption intensity at 1020 nm of $\mathbf{(C_{60}(N);ZnP)_{Rot}}$ shows the slow rise immediately after pulsed laser light excitation, whereas the quick rise was observed for $\mathbf{(C_{60}(N^+);ZnP)_{Rot}}$ as shown in Fig. 7, in which the $C_{60}^{\bullet-}$ moiety seems to rise reaching maximum at 150 ns and 50 ns after laser light excitation, respectively. This observation indicates that the CS process of $\mathbf{(C_{60}(N);ZnP)_{Rot}}$ also takes place *via* the triplet route (*via* the $^3C_{60}$* moieties). Indeed, the fractions of the ISC process competitively occurring with the CS process *via* the singlet routes are calculated from $(1 - \Phi_{CS}^{S,II})$ to be *ca.* 0.4 from the $^1C_{60}$* moiety to the $^3C_{60}$* moiety.

From the curve-fitting of the $C_{60}^{\bullet-}$-rise profile with a single exponential, the CS rate constants (k^T_{CS}) *via* the $^3C_{60}$* moiety in $\mathbf{(C_{60}(N);ZnP)_{Rot}}$ were calculated as listed in Table 4; the k^T_{CS} values were in the range of $(1.8–3.0) \times 10^7$ s^{-1}. In the case of $\mathbf{(C_{60}(N^+);ZnP)_{Rot}}$, the rise of the $C_{60}^{\bullet-}$ moiety was faster; although curve-fitting gave the k^T_{CS} values to be $(1.0–1.8) \times 10^8$ s^{-1}, they are almost within the laser light pulse width. Therefore, it is difficult to judge this rise is due to the CS process either *via* the excited singlet states or *via* the excited triplet states.

From the decay at 1020-nm band, the CR rate constants (k_{CR}) were evaluated as listed in Table 4. For $\mathbf{(C_{60}^{\bullet-}(N^+);ZnP^{\bullet+})_{Rot}}$, the k_{CR} values of $(5.4–6.1) \times 10^6$ s^{-1} are faster than those for $\mathbf{(C_{60}^{\bullet-}(N);ZnP^{\bullet+})_{Rot}}$ ($(1.8–2.5) \times 10^6$ s^{-1}) in the corresponding polar solvents. The faster k_{CR} values for $\mathbf{(C_{60}^{\bullet-}(N^+);ZnP^{\bullet+})_{Rot}}$ can be interpreted by the shorter R^{Av}_{CC}. Solvent polarity effect is not prominent, excepting $\mathbf{(C_{60}^{\bullet-}(N^+);ZnP^{\bullet+})_{Rot}}$ in toluene.

From the inverse of the k_{CR} values, the lifetimes (τ_{RIP}) of the RIPs in polar solvents were evaluated to be 400–560 ns for $\mathbf{(C_{60}^{\bullet-}(N);ZnP^{\bullet+})_{Rot}}$ and shorter τ_{RIP} values (160–180 ns) for $\mathbf{(C_{60}^{\bullet-}(N^+);ZnP^{\bullet+})_{Rot}}$, supporting the idea that the short distance between the $C_{60}^{\bullet-}$ and $ZnP^{\bullet+}$ results in short lifetimes, which is quite reasonable. In toluene, a further long τ_{RIP} value (370 ns) for $\mathbf{(C_{60}^{\bullet-}(N^+);ZnP^{\bullet+})_{Rot}}$ was observed, which is along the Marcus theory prediction, that is, the CR process belongs to the inverted region of the Marcus parabola, because the ΔG_{CR} values are larger than the reorganization energy of the $\mathbf{C_{60}}$ derivatives.[19]

Table 4 Rate constants (k_{CR}) and lifetimes (τ_{RIP}) of charge-recombination of $\mathbf{(C_{60}(N);ZnP)_{Rot}}$ and $\mathbf{(C_{60}(N^+);ZnP)_{Rot}}$ + in DMF, PhCN, THF, and toluene at room temperature

Rotaxanes	Solvent	k_{CS}^T/s^{-1a}	k_{CR}/s^{-1b}	τ_{RIP}/ns
$\mathbf{(C_{60}(N);ZnP)_{Rot}}$	DMF	3.0×10^7	2.5×10^6	400
	PhCN	2.6×10^7	2.0×10^6	500
	THF	1.8×10^7	1.8×10^6	560
$\mathbf{(C_{60}(N^+);ZnP)_{Rot}}$	DMF	$(1.0 \times 10^8)^c$	6.1×10^6	160
	PhCN	$(1.2 \times 10^8)^c$	5.5×10^6	180
	THF	$(1.4 \times 10^8)^c$	5.4×10^6	180
	TN	$(1.8 \times 10^8)^c$	2.7×10^6	370

[a] From the rise of the $C_{60}^{\bullet-}$ moiety at 1020 nm. [b] From the decay at 1020 nm. [c] Within the nanosecond laser pulse width.

Energy diagrams

Using the ΔG^S_{CS} and ΔG^T_{CS} data as well as the energy levels of the lowest excited states, the energy diagrams for both rotaxanes can be depicted. As shown in Scheme 3 for $\mathbf{(C_{60}(N);ZnP)_{Rot}}$, the CS processes to generate the RIP from the ^{1}ZnP*, ^{3}ZnP*, $^1C_{60}$* and $^3C_{60}$* moieties are possible in polar solvents; indeed, direct evidence is obtained, except for ^{3}ZnP*. The EnT process from the ^{1}ZnP* moiety is competitive with the CS process. For $\mathbf{(C_{60}(N^+);ZnP)_{Rot}}$, the excited CT state positions between the ^{1}ZnP* or $^1C_{60}$* moiety and the CS state as shown in Scheme 4; thus, the RIP is generated *via* the excited CT state after solvation. Since the excited CT state has similar energy levels to the ^{3}ZnP* or $^3C_{60}$* moieties, direct CS process is possible as evidenced by the transient absorption spectra.

The rate constants of these processes cannot be fully explained only by these energy diagrams; however, after taking the steric factors into consideration, most of the kinetic parameters including yields of the transient species can be satisfactory interpreted as shown in the text.

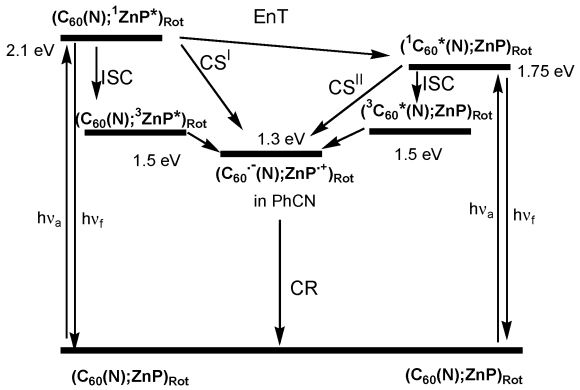

Scheme 3 Energy diagram of $\mathbf{(C_{60}(N);ZnP)_{Rot}}$ in polar solvents.

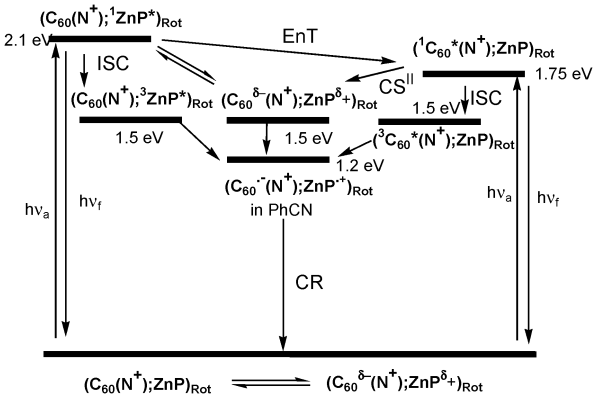

Scheme 4 Energy diagrams of $(C_{60}(N^+);ZnP)_{Rot}$ in polar solvents.

Comparison with other rotaxanes

In our previous paper,[10] we reported that the CS processes of two rotaxanes of C_{60} and Fc, $(C_{60};Fc)_{Rot}$ and $(C_{60};Fc)_{Rot+}$, in which $(C_{60};Fc)_{Rot+}$ with a shorter R_{CC}^{Av} between the C_{60} and Fc moieties has a shorter τ_{RIP} value (13 ns in PhCN) than that (30 ns) of $(C_{60};Fc)_{Rot}$ with a longer R_{CC}^{Av}.[10] This trend is in agreement with the present rotaxanes, although different axles and crown ethers were employed.

Two rotaxanes of C_{60} and triphenyl amine TPA, $(C_{60};TPA)_{Rot}$ and $(C_{6};TPA)_{Rot+}$ were also reported by us;[15] the RIPs are relatively long (τ_{RIP} = 170–300 ns in polar solvents at room temperature). $(C_{60};TPA)_{Rot+}$ has a shorter τ_{RIP} (170 ns in DMF) than that of $(C_{60};TPA)_{Rot}$ (200 ns in DMF), although the difference is small. In the case of $(C_{60};TPA)_{Rot+}$, the CT interaction between the C_{60} and TPA moieties is not appreciable, due to a different rotaxane structure (axle and crown ether).[15]

Compared with rotaxanes bearing C_{60} and bis-ZnPs in our previous report,[9] the τ_{RIP} value of $(C_{60}(N^+);ZnP)_{Rot}$ in the present study is similar to that of the short axle rotaxane, whereas the τ_{RIP} value of $(C_{60}(N);ZnP)_{Rot}$ is similar to the long axle rotaxane. These agreements indicate that the R_{CC}^{Av} values are a generally quite important factor to control the τ_{RIP} values in the rotaxanes. Furthermore, the R_{CC}^{Av} values also determine either the triplet route or the singlet route in the CS process; thus, the R_{CC}^{Av} values are important factor to determine the τ_{RIP} values.

Conclusions

For two rotaxanes in the present study, the most prominent difference between $(C_{60}(N);ZnP)_{Rot}$ and $(C_{60}(N^+);ZnP)_{Rot}$ is the CT interaction between the ZnP and C_{60} moieties in the latter rotaxane with the cationic axle, resulting in a short R_{CC}^{Av} between the two moieties. The photoinduced processes are much influenced by this CT interaction. The CS processes *via* the ^{1}ZnP* and $^1C_{60}$* moieties are slowed down by the CT interaction, even though with a shorter R_{CC}^{Av} one might anticipate a fast process. On the other hand, the CS process *via* the $^3C_{60}$* moiety and the CR process of RIPs are much accelerated with a shorter R_{CC}^{Av}. Such a difference in the ET processes may be related to the relative energy level of the excited CT state. The processes occurring from the energy levels lower than the CT state strongly depend on R_{CC}^{Av}, whereas the ET processes occurring from the energy levels higher than the excited CT state are retarded. Although the reason for this is not defined yet, the equilibrium between the ^{1}ZnP* or $^1C_{60}$* moieties and the excited CT state decelerates the apparent decay of the excited singlet state, probably because the successive conversion from the excited CT state to the CS state with solvation may not be fast, even in polar solvents.

The EnT process from the ^{1}ZnP* moiety to the C_{60} moiety is predominant in toluene; thus, the CS process *via* the ^{1}ZnP* moiety in polar solvents takes place competitively with the EnT process. In the present study, the evaluation of the relative contribution cannot be evaluated. However, as a general trend, polarity of the solvent increases the contribution of the CS process.

The longest lifetime (τ_{RIP}) of $(C_{60}^{\bullet-}(N);ZnP^{\bullet+})_{Rot}$ is realized in toluene, which is reasonable as an inverted region of the Marcus parabola. This is an advantage of $(C_{60}(N^+);ZnP)_{Rot}$ with a short R_{CC}^{Av} over $(C_{60}(N);ZnP)_{Rot}$ with a long R_{CC}^{Av}, because the prolonged RIP was not observed in the latter rotaxane in toluene.

Experimental

General

Synthesis of $(C_{60}(N^+);ZnP)_{Rot}$ has already been reported.[13] Crown-**ZnP** were prepared according to the methods described previously.[13] Other materials and solvents of reagent grade were used without further purification. IR spectra were recorded on a JASCO FT-IR model 230 spectrometer. ^{1}H and ^{13}C NMR measurements were performed on JEOL JNM-GX-270 and JNM-L-400 spectrometers in $CDCl_3$ with tetramethylsilane as an internal reference. MALDI-TOF-MS measurements were performed on a AXIMA-CFR mass spectrometer. Steady-state absorption spectra in the visible and near-IR regions were measured on a Jasco V570 DS spectrometer. Fluorescence spectra were measured on a Shimadzu RF-5300PC spectro-fluorophotometer.

Synthesis of $(C_{60}(N);ZnP)_{Rot}$

To a solution of $(C_{60}(N^+);ZnP)_{Rot}$ (40 mg, 15 μmol) in CD_3CN–$CDCl_3$ (0.60 mL/0.3 mL) were added benzoyl chloride (20 μL, 100 μmol) and triethylamine (30 μL, 210 μmol) in the dark. The mixture was stirred at 50 °C for 22 h. The reaction mixture was evaporated, and the residue was dissolved in $CHCl_3$. The solution was washed with saturated aqueous $NaHCO_3$ and brine, dried over anhydrous $MgSO_4$, filtered, and evaporated to dryness. The residue was subjected to silica gel column chromatography (eluent: $CHCl_3$) to afford $(C_{60}(N);ZnP)_{Rot}$ as a black purple solid (30 mg, 76%). ^{1}H-NMR (400 MHz, $CDCl_3$, 333 K) δ 9.23 (s, 1H), 8.95–8.86 (m, 7H), 8.69 (br, 1H), 8.09–7.94 (m, 10H), 7.79 (s, 3H), 7.65–7.27 (m, 12H), 6.87–6.78 (m, 10H), 6.06–6.01 (m, 2H), 4.53–3.03 (m, 32H), 2.29–2.26 (m, 6H), 1.53–1.44 (m, 54H) ppm. IR (NaCl) 2961, 1715, 1504, 1682, 1591, 1504, 1454, 1362, 1265, 1126, 1001, 797, 716, 527 cm^{-1}. UV-vis λ_{max}/nm (ε/M^{-1} cm^{-1}) ($CHCl_3$): 425.5 (420 000), 552.0 (17 000), 592.0 (5800). MALDI-TOF-MS (matrix; Dithranol) m/z 2711.0

(calcd for $C_{186}H_{138}N_6O_{12}Zn$ = 2711.0). Anal. calcd for $C_{186}H_{138}N_6O_{12}Zn\cdot(CHCl_3)_{0.75}$: C, 79.99; H, 4.99; N, 3.00%. Found: C, 79.60; H, 5.40; N, 3.13%.

Spectral measurements

The time-resolved fluorescence spectra were measured by single-photon counting method using the second harmonic generation (SHG, 410 nm) of a Ti:sapphire laser [Spectra-physics, Tsunami 3950-L2S, 1.5 ps full width at half-maximum (fwhm)] and a streak scope (Hamamatsu Photonics, C4334-01) equipped with a polychromator (Action Research, SpectraPro 150) as excitation source and detector, respectively.

Nanosecond transient absorption measurements were carried out using the SHG (532 nm) of an Nd:YAG laser (Spectra Physics, Quanta-Ray GCR-130, fwhm 6 ns) as excitation source. For the transient absorption spectra in the near-IR region (600–1600 nm), the monitoring light from a pulsed Xe lamp was detected with a Ge-avalanche photodiode (Hamamatsu Photonics, B2834). The photoinduced events in micro- and millisecond time regions were estimated using a continuous Xe lamp (150 W) and an InGaAs-PIN photodiode (Hamamatsu Photonics, G5125-10) as probe light and detector, respectively. The details of the transient absorption measurements were described elsewhere.[20] All the samples in a quartz cell (1 × 1 cm) were deaerated by bubbling argon through the solution for 15 min.

Electrochemical measurements

The cyclic voltammetry measurements were performed on a BAS CV-50 W electrochemical analyzer in deaerated PhCN solution containing 0.10 M Bu_4NPF_6 as a supporting electrolyte at 298 K (100 mV s^{-1}). The glassy carbon working electrode was polished with BAS polishing alumina suspension and rinsed with acetone before use. The counter electrode was a platinum wire. The measured potentials were recorded using an Ag/AgCl (saturated KCl) electrode as reference electrode.

Acknowledgements

This present work was supported by a Grant-in-Aid on Scientific Research on Priority Areas (417) from the Ministry of Education, Culture, Sports, Science and Technology of Japan (12875163 and 14050014).

References

1 C. O.-D. Buchecker and J.-P. Sauvage, *Chem. Rev.*, 1987, **87**, 795; J.-M. Lehn, *Supramolecular Chemistry*, Wiley-VCH, Weinheim, 1995; J.-P. Sauvage and C. O.-D. Buchecker, *Molecular Catenanes, Rotaxanes and Knots*, Wiley-VCH, Weinheim, 1999; V. Balzani, M. Venturi and A. Credi, *Molecular Devices and Machines*, Wiley-VCH, Weinheim, 2003.
2 J. R. Heath, *Acc. Chem. Res.*, 1999, **32**, 388; E. A. Chandross and R. D. Miller, *Chem. Rev.*, 1999, **99**, 1641; M. Schultz, *Nature*, 1999, **399**, 729; R. Dagani, *Chem. Eng. News*, 2000, **78**, 22; P. F. Barbara, *Acc. Chem. Res.*, 2001, **34**, 409; R. Ballardini, V. Balzani, M. Clemente-León, A. Credi, M. T. Gandolfi, E. Ishow, J. Perkins, J. F. Stoddart, H.-R. Tseng and S. Wenger, *J. Am. Chem. Soc.*, 2002, **124**, 12786.
3 A. Andersson, M. Linke, J.-C. Chambron, J. Davidsson, V. Heitz, J.-P. Sauvage and L. Hammarstrom, *J. Am. Chem. Soc.*, 2000, **122**, 3526; A. Andersson, M. Linke, J.-C. Chambron, J. Davidsson, V. Heitz, J.-P. Sauvage and L. Hammarstrom, *J. Am. Chem. Soc.*, 2002, **124**, 4347.
4 *Introduction of Molecular Electronics*, ed. M. C. Petty, M. R. Bryce and D. Bloor, Oxford University Press, New York, 1995; *Molecular Switches*, ed. B. L. Feringa, Wiley-VCH GmbH, Weinheim, 2001.
5 D. M. Guldi, J. Ramey, M. V. Martinez-Diaz, A. de la Escosura, T. Torres, T. Da Ros and M. Prato, *Chem. Commun.*, 2002, 2774; A. Matero-Alonso, G. Fiaoravanti, M. Marcaccio, F. Paolucci, D. C. Jagesar, A. M. Brouwe and M. Prato, *Org. Lett.*, 2006, **8**, 5171; A. Matero-Alonso, G. M. A. Rahman, C. Ehli, D. M. Guldi, G. Fioravant, M. Marcaccio, F. Paolucci and M. Prato, *Photochem. Photobiol. Sci.*, 2006, **5**, 1173; A. Matero-Alonso, D. M. Guldi and M. Prato, *Angew. Chem., Int. Ed.*, 2007, **46**, 8120.
6 F. Diederich, C. Dietrich-Buchecker, J.-F. Nierengarten and J.-P. Sauvage, *J. Chem. Soc., Chem. Commun.*, 1995, 781; N. Solladie, M. E. Walther, M. Gross, T. M. Figueira Duarte, C. Bourgogne and J.-F. Nierengarten, *Chem. Commun.*, 2003, 2412.
7 N. Watanabe, N. Kihara, Y. Furusho, T. Takata, Y. Araki and O. Ito, *Angew. Chem., Int. Ed.*, 2003, **42**, 681.
8 D. I. Schuster, K. Li, D. M. Guldi and J. Ramey, *Org. Lett.*, 2004, **6**, 1919; K. Li, D. I. Schuster, D. M. Guldi, M. A. Herranz and L. Echegoyen, *J. Am. Chem. Soc.*, 2004, **126**, 3388.
9 A. S. D. Sandanayaka, N. Watanabe, K. Ikeshita, Y. Araki, N. Kihara, Y. Furusho, O. Ito and T. Takata, *J. Phys. Chem. A*, 2004, **109**, 2516.
10 A. S. D. Sandanayaka, H. Sasabe, Y. Araki, K. Kihara, Y. Furusho, T. Takata and O. Ito, *Aust. J. Chem.*, 2006, **59**, 186.
11 Y. Araki and O. Ito, *J. Photochem. Photobiol., C*, 2008, **9**, 93.
12 F. D'Souza and O. Ito, *Chem. Commun.*, 2009, 4913.
13 M. Maes, H. Sasabe, N. Kihara, Y. Araki, Y. Furusho, K. Mizuno, T. Takata and O. Ito, *J. Porphyrins Phthalocyanines*, 2005, **9**, 724; H. Sasabe, Y. Furusho, A. S. D. Sandanayaka, Y. Araki, N. Kihara, K. Mizuno, A. Ogawa, O. Ito and T. Takata, *J. Porphyrins Phthalocyanines*, 2006, **10**, 1346; H. Sasabe and T. Takata, *J. Porphyrins Phthalocyanines*, 2007, **11**, 334.
14 *GAUSSIAN 03 (Revision A.7)*, Gaussian, Inc., Pittsburgh, PA, 2003 (see the ESI† for the full reference).
15 A. S. D. Sandanayaka, H. Sasabe, Y. Araki, Y. Furusho, O. Ito and T. Takata, *J. Phys. Chem. A*, 2004, **108**, 5145.
16 D. Rehm and A. Weller, *Ber. Bunsenges Phys. Chem.*, 1969, **73**, 834; A. Weller, *Z. Phys. Chem. Neue Folge*, 1982, **133**, 93; N. Mataga and H. Miyasaka, in *Electron Transfer*, ed. J. Jortner and M. Bixon, John Wiley & Sons, New York, 1999, Part 2, pp. 431–496.
17 H. Imahori, N. V. Tkachenko, V. Vehmanen, K. Tamaki, H. Lemmetyinen, Y. Sakata and S. Fukuzumi, *J. Phys. Chem. A*, 2001, **105**, 2175; V. Chukharev, N. V. Tkachenko, A. Efimov, D. M. Guldi, A. Hirsh, M. Scheloske and H. Lemmetyinen, *J. Phys. Chem. B*, 2004, **108**, 16377.
18 J. R. Lakowicz, *Principles of Fluorescence Spectroscopy*, Plenum Press, New York, 2nd edn, 2001.
19 R. A. Marcus, *J. Chem. Phys.*, 1956, **24**, 966; R. A. Marcus, *J. Chem. Phys.*, 1965, **43**, 679; R. A. Marcus and N. Sutin, *Biochim. Biophys. Acta*, 1985, **811**, 265.
20 Y. Araki and O. Ito, in *Handbook of Organic Electronics and Photonics*, ed. H. S. Nalwa, American Scientific Publishers, California, 2008, ch. 12, vol. 2, pp. 473–513.